

# Faraday-Talbot Effect from a Circular Array of Pillars

J.J. Pilgram and N. Sungar\*

*Department of Physics, California Polytechnic State University,  
San Luis Obispo, California 93407, USA*

L.D. Tamasco and J.W. Bush

*Department of Mathematics,  
Massachusetts Institute of Technology,  
Cambridge, Massachusetts 02139, USA*

(Dated: November 28, 2017)

When an oil bath is vertically oscillating with an acceleration above some critical value, known as the Faraday threshold, the bath surface becomes unstable and nonlinear standing wave patterns emerge. One phenomenon that has been observed above the Faraday threshold is the formation of Faraday-Talbot carpets, resulting from near-field diffraction. The optical Talbot effect occurs when a monochromatic wave passes through a diffraction grating. In the near-field, the formation of self-images is observed at integer multiples of what is known as the Talbot length. These two-dimensional patterns have various applications including X-ray imaging and atom and particle trapping. Two-dimensional Faraday-Talbot wave patterns have been observed in an oil bath oscillating above the Faraday threshold containing a row of evenly spaced, protruding pillars. These pillars generate sloshing waves which serve as active sources of monochromatic Faraday waves, the interference of which generates the Faraday-Talbot wave patterns. These patterns were observed to trap bouncing and walking droplets at the location of the pillar images. As an extension of the two-dimensional linear Faraday-Talbot effect, we present novel stable and transient Faraday-Talbot carpets created from a circular array of evenly spaced pillars. An understanding of the formation of stable Faraday-Talbot carpets can act as an analogy to atom and particle trapping and may provide insights into particle trapping mechanisms.

## I. INTRODUCTION

When the free surface of an oil bath is vertically oscillated with an amplitude,  $A$ , frequency,  $f$ , and a sufficient acceleration,  $\Gamma(t) = \gamma \cos(2\pi ft)$ , the surface becomes unstable and standing wave patterns form with a frequency of  $f/2$  [1]. The acceleration at which these standing wave patterns begin to form is known as the Faraday threshold,  $\gamma_F$ . For vibrational acceleration  $\gamma = A(2\pi f)^2$  where  $\gamma < \gamma_F$  the fluid surface is stable and no wave patterns can form as all excitations decay. However when  $\gamma > \gamma_F$ , unstable subharmonic Faraday waves with a wavelength of  $\lambda_F = 2\pi/k_F$  form on the fluid surface. These waves are described by the water-wave dispersion relation

$$\omega^2(k) = (gk + \frac{\sigma}{\rho}k^3)\tanh(hk) \quad (1)$$

where  $k$  is the wavenumber,  $g$  is the gravitational acceleration constant,  $\sigma$  is the surface tension,  $\rho$  is the fluid density and  $h$  is the fluid depth.

Faraday waves have been studied both experimentally and theoretically and have been used to study hydrodynamic quantum analogs [2]. Faraday waves can act as

optical analogs as well such as the Talbot effect.

The optical Talbot effect is a result of near field diffraction that occurs when a monochromatic wave, of wavelength  $\lambda$ , is passed through a periodic grating [3]. This effect was discovered in 1836 by Henry Fox Talbot by examining optical patterns behind a diffraction grating [4] and the theory was later developed by Lord Rayleigh in 1881 [5]. The theory expresses the intensity pattern resulting from the interference of waves from individual slits as a sum of monochromatic plane waves of wavelength  $\lambda$  with transverse wave-vector components  $2\pi n/d$ , where  $d$  is the slit spacing and  $n$  is an integer. At integer multiples of a distance,  $z_t$ , perpendicular to the grating, direct images of the grating are reproduced. This distance is known as the Talbot length, is given by

$$z_t(\lambda) = \frac{\lambda}{2(1 - \sqrt{1 - (\frac{\lambda}{d})^2})} \quad (2)$$

At even multiples of the Talbot length, the self-images are spatially in-phase with the grating and at odd integer multiples the images are shifted by half of the slit spacing,  $d/2$  [6].

The Talbot effect has been studied and applied in a variety of optical systems [7, 8] and has applications in

---

\* nsungar@calpoly.edu

phenomena such as optical trapping of atoms [9] and particles [10], atom wave interference [11], Bose-Einstein condensates [12], plasmonics [13] and X-ray imaging [14]. Not only has the Talbot effect been studied and applied optically, it has been recently observed in a hydrodynamic system. Sungar et al. [15] observed and studied the formation of Faraday-Talbot carpets on a vertically oscillating oil surface as a result of an array of evenly spaced pillars in the bath. These patterns are observed to form only when the spacing of the pillars is either an integer or half-integer multiple of the Faraday wavelength. The source of the patterns were determined as sloshing inter-pillar ridges of fluid that form in between the pillars. When the pillar spacing is an integer multiple of the Faraday wavelength,  $\lambda_F$ , the ridges in between the pillars oscillate in-phase and the Talbot wave pattern has self-images given by equation 2. When the pillars spacing is half-integer multiples of  $\lambda_F$ , the ridges in between the pillars are alternately out of phase and a different variety of Talbot pattern appears. This is referred to as the alternate phase Talbot effect. In this case, calculations show [16] that the Talbot length is given by

$$z_t(\lambda) = \frac{\lambda}{\sqrt{1 - \frac{\lambda^2}{4d^2}} - \sqrt{1 - \frac{9\lambda^2}{4d^2}}} \quad (3)$$

Experiments studying the formation of Talbot carpets from a curved diffraction grating conducted by Wei Zhang et al [17] revealed that the periodicity of the self-images, ie. the spacing between each consecutive image in any given row of self-images is either magnified or demagnified relative to the periodicity of the grating. Magnification occurs when the images are viewed on the convex side of the grating and demagnification occurs on the concave side of the grating. In comparison to the periodicity of a linear grating, this magnified periodicity,  $P$ , of images is given by:

$$P = \frac{R}{R - nz_T}d \quad (4)$$

Where  $n$  is an integer,  $z_T$  is the Talbot length given by equation 2 or 3, and  $R$  is the radius of curvature of the diffraction grating, and  $d$  is slit spacing. For the alternate phase Talbot effect, a slit spacing of  $2d$  must be used because the array is considered to be the superposition of two interlaced sub-arrays, each in itself coherent but opposite in phase to the other sub-array each having the periodicity of  $2d$ .  $R$  is positive for images on the convex side of the grating and negative for images on the concave side of the grating.

Here we present an experimental and computational study of Faraday-Talbot carpets from a circular array of pillars for both varieties of Talbot patterns, when the ridges oscillate in phase and out of phase.

## II. SIMULATIONS

First, simulations of Talbot-carpet patterns formed from a circular array of pillars were created using MatLab scripts. The script intakes parameters for the vertical oscillation frequency, number of pillars and the integer multiple of the wavelength that the pillars will be spaced. The program then calculates the wavenumber for a given set of constants such as the fluid density and surface tension by solving equation 1 which is then used to calculate the wavelength of the Faraday waves.

From the geometry of the system it is determined that the radius of the circle of pillars should be given by

$$r = \frac{m\lambda/2}{\sin(\pi/n)} \quad (5)$$

Where  $\lambda$  is the Faraday wavelength,  $m$  denotes the multiple of the wavelength for which the pillars are to be spaced, and  $n$  is the number of pillars. Arrays consisting of the  $x$  and  $y$  coordinates of the pillars are created by solving for the vertices of an  $n$  side polygon of radius  $r$  given by equation 5.

In the simulations, for each time-step, the program calculates at each spacial point in the plane the amplitude of the the surface waves by summing the wave contributions from each source. These wave amplitudes at all spacial points for each time-step are then compiled into a video using MATLAB videowriter and are saved as a .avi file that can be viewed and analyzed in any compatible video player. The program code is displayed in Appendix A.

## III. EXPERIMENTAL APPARATUS

The experimental set up consisted of an electromagnetic shaker vertically oscillating a 180 mm diameter circular oil bath, filled with 20 cS silicone oil to a depth of 4-5 mm. A base plate consisting of a circle of  $N$  protruding, 3 mm diameter plastic pillars, spaced at a distance  $d = n\lambda_f$  where  $n$  is either an integer or half-integer. The radius of the circular array was determined by simulations described earlier. The bath was then vertically shaken at a forcing frequency of either 80 or 55 Hz and the forcing acceleration was increased until Faraday waves were visible. A semi-reflective mirror was placed above the oil bath at an angle of 45 degrees below the horizontal. With illumination from the side, video images of the resulting patterns were recorded via a high speed camera mounted directly above the mirror. A schematic of the experimental set up is displayed in Figure 1.

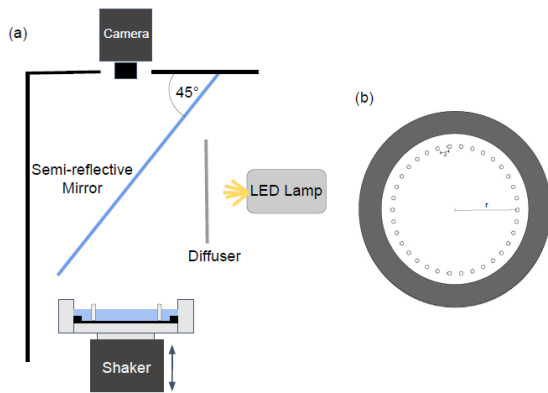


FIG. 1. (a) Side view of the experimental setup. (b) Top view of oil bath with  $N$  protruding, 3 mm diameter pillars evenly spaced at a distance  $d$ , at a radius  $r$  from the center.

#### IV. EXPERIMENTAL RESULTS

A variety of circular arrays were tested at forcing frequencies of both 80 and 55 Hz. The forcing acceleration of the bath was set above the Faraday threshold,  $\gamma_F$ , and the resulting surface patterns were recorded. Patterns were observed to form for a 51.5 mm radius circular array of 34 pillars. The pattern observed at a forcing frequency of 80 Hz was determined to be the standard Talbot effect and the pattern observed at a forcing frequency of 55 Hz was determined to be the alternate phase Talbot effect. The videos were viewed and analyzed using MATLAB video viewer and the MATLAB image viewer distance measuring tool.

The separation distances between adjacent images in each circular row were measured and compared to the theoretical values given by equation 4. The experiment is in good agreement with the theory, most values falling within two or three standard deviations. Both experimental and theoretical values are displayed in Table I.

Although the experimentally observed patterns are in good agreement with both simulations and theoretical values, only one of the observed patterns was stable. This was the pattern observed with the 51.5 mm radius array of 34 pillars at a forcing frequency of 55 Hz, shown in Figure 3. The observed pattern at a forcing frequency of 80 Hz, shown in Figure 2, was transient, decaying within one minute of initial pattern formation. It is believed that the equilibrium state for which this pattern forms is unstable, thus any minute deviation or imperfection in the system causes the patterns to decay. It is possible that with a circular array of sources, the patterns for the standard Talbot effect are unstable but patterns for the alternate phase Talbot effect are stable. Further experiments should be conducted using a variety of other circular arrays in order to test this hypothesis.

	R(mm)	$\lambda_F$ (mm)	$z_T$ (mm)	$n$	$P_{th}$ (mm)	$P_{exp}$ (mm)
80 Hz:						
$d = 9.5$	51.5	4.75	17.73	1	7.07	$6.81 \pm 0.21$
$d = 9.5$	51.5	4.75	17.73	2	5.63	$5.66 \pm 0.25$
$d = 9.5$	51.5	4.75	17.73	3	4.67	$4.77 \pm 0.17$
55 Hz:						
$d = 9.5$	51.5	6.33	6.95	2	14.96	$15.76 \pm 0.33$
$d = 9.5$	51.5	6.33	6.95	4	12.34	$12.56 \pm 0.28$
$d = 9.5$	51.5	6.33	6.95	6	10.50	$7.31 \pm 0.29$

TABLE I. System parameters and theoretical and experimental values of the magnification factor,  $P_{th}$  and  $P_{exp}$ .  $d$  is the spacing between the pillars,  $R$  is the radius of the circular array,  $\lambda_F$  is the Faraday wavelength,  $z_t$  is the Talbot length, and  $n$  is an integer denoting the circle of images with 1 being the outer most circle.

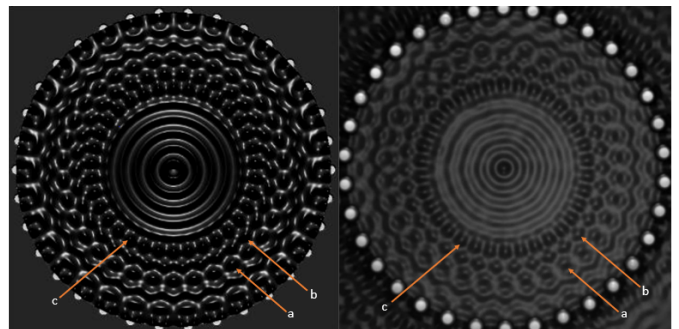


FIG. 2. **Left:** Simulation for a 51.5 mm radius circular array of 34 pillars, spaced at a distance of 9.5 mm at a forcing frequency of 80 Hz. **Right:** Experimentally observed pattern with a vertical acceleration of 4.33g. **a** displays the first circle of images, **b** denotes the second circle of images, and **c** denotes the third and inner most circle of images.

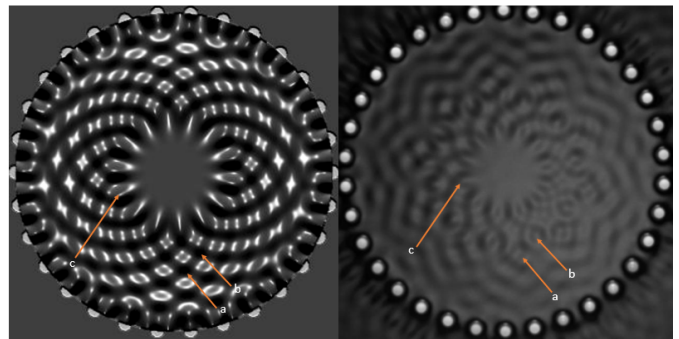


FIG. 3. **Left:** Simulation for a 51.5 mm radius circular array of 34 pillars, spaced at a distance of 9.5 mm at a forcing frequency of 55 Hz. **Right:** Experimentally observed pattern with a vertical acceleration of 2.23g. **a** displays the first circle of images, **b** denotes the second row of images, and **c** denotes the third and inner most circle of images.

## V. CONCLUSION

Experiments were conducted to examine Faraday-Talbot carpets from a circular array of evenly spaced, protruding pillars. Patterns were observed and agree with simulations and theoretical values for a 51.5 mm radius array of 34 pillars at forcing frequencies of both 55 and 80 Hz. The Talbot carpet observed from 34 pillar array at 55 Hz was very stable. However, the Talbot carpet observed at 80 Hz was transient, decaying within one minute of initial formation, possibly a result of the unstable equilibrium state for these patterns. A more extensive study of the Faraday-Talbot wave theory should be conducted for better understanding of the mechanisms behind the transient behavior of these patterns. Additionally, further experiments should be conducted to determine if, for circular arrays, all patterns for the alternate phase Talbot effect are stable

where as patterns for the standard Talbot effect are not. Understanding and creating stable Talbot carpets could provide a mechanism for droplet trapping which would act as an analogy to optical atom trapping. Additionally, stable Talbot carpets may potentially be used as a mechanism for fluid transport and drug delivery in digital microfluidic systems.

## VI. ACKNOWLEDGEMENTS

The authors would like to thank the California Polytechnic State University, San Luis Obispo department of physics, the Massachusetts Institute of Technology department of mathematics, and the Massachusetts Institute of Technology General Summer Research Program for the financial and general support of this research. The MIT applied mathematics lab is funded by the National Science Foundation.

- 
- [1] M. Faraday, Philosophical transactions of the Royal Society of London **121**, 299 (1831).
  - [2] J. W. Bush, Physics Today **68**, 47 (2015).
  - [3] K. Paturski and E. Wolf, (1989).
  - [4] H. F. Talbot, The London and Edinburgh Philosophical Magazine and Journal of Science **9**, 401 (1836).
  - [5] Rayleigh, Phil. Mag. **11** (1881).
  - [6] W. B. Case, M. Tomandl, S. Deachapunya, and M. Arndt, "Realization of optical carpets in the talbot and talbot-lau configurations," (2009).
  - [7] J. Wen, Y. Zhang, and M. Xiao, Advances in Optics and Photonics **5**, 83 (2013).
  - [8] M. V. Berry and S. Klein, Journal of modern optics **43**, 2139 (1996).
  - [9] R. Newell, J. Sebby, and T. Walker, Optics letters **28**, 1266 (2003).
  - [10] Y. Sun, X.-C. Yuan, L. Ong, J. Bu, S. Zhu, and R. Liu, Applied physics letters **90**, 031107 (2007).
  - [11] M. S. Chapman, C. R. Ekstrom, T. D. Hammond, J. Schmiedmayer, B. E. Tannian, S. Wehinger, and D. E. Pritchard, Physical Review A **51**, R14 (1995).
  - [12] L. Deng, E. W. Hagley, J. Denschlag, J. Simsarian, M. Edwards, C. W. Clark, K. Helmerson, S. Rolston, and W. D. Phillips, Physical Review Letters **83**, 5407 (1999).
  - [13] W. Zhang, C. Zhao, J. Wang, and J. Zhang, Optics express **17**, 19757 (2009).
  - [14] T. Weitkamp, A. Diaz, C. David, F. Pfeiffer, M. Stambanoni, P. Cloetens, and E. Ziegler, Optics express **13**, 6296 (2005).
  - [15] N. Sungar, L. Tambasco, G. Pucci, P. Sáenz, and J. Bush, Physical Review Fluids **2**, 103602 (2017).
  - [16] N. Sungar, In Preparation. For more information contact: nsungar@calpoly.edu.
  - [17] W. Zhang, J. Wang, Y. Cui, and S. Teng, Optics Communications **341**, 245 (2015).

## APPENDIX A

This section contains the MATLAB code used to create simulations of Talbot carpets on a two dimensional surface from an evenly spaced circular array of sources.

---

```

%function parameters: f = forcing frequency
%p = number of pillars
%in = 1 or -1 (1 for in-phase -1 for out-of-phase)
%if doing out of phase you must hard set the radius of the circle in the function code*
%res = resolution of video (I have been using 1)
%m = integer multiple of wavelength for pillar spacing (d = m*lam)

function out = Talbot_patterns(f,p,in,res,m)
f1=f/2; %faraday freq
w=2*pi*f1;
g = 9810; %g in mm/s^2
rho = 0.949*10^-3; %density
sig = 20.6; %surface tension
h = 4; %depth in mm either 4,5,or 6

kf=fzero(@(k) (g*k+sig/rho*k.^3).*tanh(k*h)-w^2,1); %wavenumber
lam=2*pi/kf %faraday wavelength

r1 = (m/2)*lam/sin(pi/p) %radius of circle

b = p/2; %half the number of pillars
q = 0:1:p;
theta = pi/b + pi/b*q; %angle position of each pillar
x1 = r1*cos(theta); % x-coord of pillar
y1 = r1*sin(theta); % y-coord of pillar

c1 = 1i*2*pi/lam;
c2 = 1i*2*pi*f1; %angular frequency of Faraday waves
x = -(r1+3):res:(r1+3); %creates array consisting of x-coord points in field of interest
y = -(r1+3):res:(r1+3); %creates array consisting of y-coord points in field of interest

t = 0:2*pi/(w*32):2*pi/w; %time steps for simulation based on periodicity
%create file name:
file = ['Talbot_f=',num2str(f),'_p=',num2str(p),'_r=',num2str(r1),'_m=', num2str(m)]
writerObj = VideoWriter([file, '.avi']); % creates a file to write a video
writerObj.FrameRate=2; % sets the playback frame rate for the video
open(writerObj);

for l = 1:size(t,2) %loop for timesteps
    F = zeros(size(x,2),size(y,2)); %setting a blank array for amplitude displacements
    for k= 1:size(x,2) %looping over x-coordinates
        for j = 1:size(y,2) %looping over y-coordinates
            sum1 = 0; %initializing sum
            dist = sqrt(x(k)^2 + y(j)^2); %distance from source to point of interest (POI)
            for n=1:p %looping over of sources
                if dist < r1 %only calculating values inside of circle
                    r = sqrt((x(k)-x1(n))^2+(y(j)-y1(n))^2); %distance from source to POI
                    sum1=sum1+exp(c1*r)/sqrt(r)*exp(-c2*t(l))*in^n; %sums all contributions
                else if dist >= r1 && dist < (r1+3) %this else statement creates pillar images
                    r = sqrt((x(k)-x1(n))^2 + (y(j)-y1(n))^2);
                    if r < 1.5

```

```

                                sum1 = 10;
                            end
                        end
                    end
                end
            F(k,j) = real(sum1) %takes only the real part of the sum
        end
    end

[X,Y]=meshgrid(x,y);
h=surf(X,Y,F'); % add 1 in here
axis equal      % fixes the axis so x and z directions are on the same scale
colormap(gray)

%the next commands adjust appearance of plot so it's observed and lighted from the top
view(2)
shading interp
lightangle(0,45) %sets angle of light source
h.FaceLighting = 'gouraud';
h.AmbientStrength = 0;
h.DiffuseStrength = 0.9;
h.SpecularStrength = 0.7;
h.SpecularExponent = 9.9;
h.BackFaceLighting = 'unlit';

drawnow
frame = getframe; % writes each plot into the video file
writeVideo(writerObj, frame);
end
close(writerObj); % closes the video file
end

```

---